Single Phase Fluid Flow in Series of Microchannel Connected via Converging-Diverging Section with or without Throat

Abhishek Kumar Chandra, Kaushal Kishor, Wasim Khan, Dhananjay Singh, M. S. Alam

Abstract—Single phase fluid flow through series of uniform microchannels connected via transition section (converging-diverging section with or without throat) was analytically and numerically studied to characterize the flow within the channel and in the transition sections. Three sets of microchannels of diameters 100, 184, and 249 μm were considered for investigation. Each set contains 10 numbers of microchannels of length 20 mm, connected to each other in series via transition sections. Transition section consists of either converging-diverging section with throat or without throat. The effect of non-uniformity in microchannels on pressure drop was determined by passing water/air through the set of channels for Reynolds number 50 to 1000. Compressibility and rarefaction effects in transition sections were also tested analytically and numerically for air flow. The analytical and numerical results show that these configurations can be used in enhancement of transport processes. However, converging-diverging section without throat shows superior performance over with throat configuration.

Keywords—Contraction-expansion flow, integrated microchannel, microchannel network, single phase flow.

I. INTRODUCTION

IN the early 80s, large scale integration technique came into existence in complex electronic circuits, containing several individual components, which dramatically improve the functionality and capability of electronic circuits. Similar system integration technique offered by the microfluidic system such as simple microchannel network with functional microfluidic modules enables execution, control, and automation of complicated chemical and biological operations in a single device. This technique intensifies the mixing, heat and mass transfer, and reaction in the microfluidic system and offers long-term benefits of resource conservation and environmental protection. In the past, numerous efforts have been made especially for fluid flow and heat transfer in single or parallel microchannels due to their wide application in micro heat exchange processes, microreactor, fuel cells, biomedical devices, etc. However, most of these studies [1]-[5] reported that the measured mass flow rate and pressure distribution in the channel show the development of slip flow near the wall. The major pressure loss in these channels is due to friction.

In the microchannel network, minor loss is present in the microfluidic system due to variety of elements such as bends, branching or contraction/expansion transitions in all internal fluidic systems. In many cases, these losses are negligible in comparison to major pressure losses, although in other cases the minor losses cannot be neglected and are responsible for a large pressure drop. Several researchers have systematically studied the minor pressure losses in microchannel system owing bend [6], gradual transitions [7], constriction elements [8], [9], and mixing [10], [11]. Further, the effects of sudden contraction and fluid rheology on the fluid characteristics were studied and reviewed [12], [13]. Two similar microchannels of different diameter, connected in series with the connection having an included angle of 5°, 15°, 90°, and 180° were studied to examine the effect of mass flow rate on pressure drop [14]. They found significantly higher pressure drop at the junction of the channels.

As seen from the above literature review, it was observed that fluid flow and heat transfer in set of microchannel connected in series via a variety of configuration have not received much attention although the flow through these configurations differs substantially from the uniform cross-section counterparts. These issues provide the motivation for the present work. Therefore, focus has been given to single phase fluid flow behaviour in such a channel. In the present study, 3D CFD simulations were used to examine the fluid dynamics in circular microchannels (diameter=100 μm and length=20 mm) connected to each other in series via transition section viz. converging-diverging section, converging-diverging with throat section. This study reveals the better design of various microflow devices.

II. MODEL FOR MICROCHANNEL

To achieve the key objectives both analytical and numerical techniques have been utilized to obtain precise and consistent data. A schematic diagram of the microchannel system along with connection elements is shown in Fig. 1. Three microchannels of hydraulic diameters 100, 184, and 249 μm were considered in this investigation are presented in Table I. Microchannels of equal diameter are connected in series, consists 10 numbers of microchannels of 20 mm length, via transition sections. Two types of transition sections (converging-diverging section and converging-diverging sections with throat, as shown in Fig. 1) were used to connect

Abhishek Kumar Chandra, Kaushal Kishor and Wasim Khan are with the Department of Chemical Engineering, Motilal Nehru National Institute of Technology, Allahabad, U.P. India (e-mail: abhishek_chandra@rediffmail.com, kk2kaushal@gmail.com, wsmkhan03@gmail.com).

M. S. Alam is with the Department of Chemical Engineering, Motilal Nehru National Institute of Technology, Allahabad, U.P. India (corresponding author, e-mail: msalam@mnnit.ac.in).

Dhananjay Singh is with the Department of Chemical Engineering, Institute of Engineering &Technology, Lucknow, U.P. India.

the microchannels. Cross-section of connection elements varies along the flow direction and having gradual and sharp corners. The angles of converging/diverging sections are 2.3°, and 4.6° for without and with throat, respectively. All the three microchannel were analysed over a Reynolds number range of 50 to 1000.

TABLE I
GEOMETRIC SPECIFICATION OF DIFFERENT MICROCHANNEL WITH CHANNEL DIMENSION

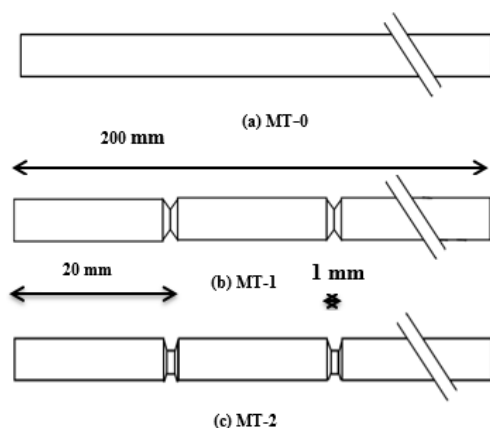| Sr. No.	Channel Notation	Diameter, m	Minimum diameter (at the junction/throat), m	Length of channel (including transition section), cm	Converging/ diverging angle	Length of transition section, mm
1	MT-0	100	-	20	-	-
		184	-			
		249	-			
2	MT-1	100	60	20	2.3 °	1
		184	110			
		249	150			
3	MT-2	100	60	20	4.6°	1

Fig. 1 Schematic diagram of the microchannels (a) MT-0 [Plain microchannel], (b) MT-1 [Microchannels connected via converging-diverging section], (c) MT-2 [Microchannels connected via converging-diverging section with throat]

A. Model for the Microchannel with Converging-Diverging Elements

The cross sectional area of flow varies linearly with the distance along the z direction in the transition section. In the flow field analysis, the following assumptions were made:

- The flow is steady, three dimensional, and locally fully developed.
- The flow is laminar for all velocity range.
- No slip condition at the wall was applied for liquid flow while for gas flow velocity slip assumption was used.
- The transport processes are considered to be steady.
- Gravity effects are negligible at such scale.

In addition, it has also been considered that velocity at the entrance of transition (converging-diverging) section i.e., $z = 0$, reaches to fully developed state and the velocity can be obtained by correlation, $v_z = 2 < v_{z=0} > \left[1 - \left(\frac{r}{r_0}\right)^2\right]$, where $< v_{z=0} >$ is the average fluid axial velocity and r_0 channel radius, (m). In the transition (converging-diverging) section flow varies linearly with the distance z in the direction of flow, but the flow remains axis-symmetric about the z-axis.

General continuity and momentum equations (Navier-Stokes equations) for three-dimensional fluid flow through circular channel are represented below which can be reorganized to obtain governing equations for the microchannel used in this investigation:

Continuity equation:

$$\frac{\partial \rho}{\partial t} + \frac{1}{r}\frac{\partial}{\partial r}(\rho r v_r) + \frac{1}{r}\frac{\partial}{\partial \theta}(\rho v_\theta) + \frac{\partial}{\partial z}(\rho v_z) = 0 \qquad (1)$$

Equation of motion:

$$\rho\left(\frac{\partial v_r}{\partial t} + v_r\frac{\partial v_r}{\partial r} + \frac{v_\theta}{r}\frac{\partial v_r}{\partial \theta} - \frac{v_\theta^2}{r} + v_z\frac{\partial v_r}{\partial z}\right) = -\frac{\partial p}{\partial r} + \mu\left[\frac{\partial}{\partial r}\left(\frac{1}{r}\frac{\partial}{\partial r}(r v_r)\right) + \frac{1}{r^2}\frac{\partial^2 v_r}{\partial \theta^2} - \frac{2}{r^2}\frac{\partial v_\theta}{\partial \theta} + \frac{\partial^2 v_r}{\partial z^2}\right] \qquad (2)$$

$$\rho\left(\frac{\partial v_z}{\partial t} + v_r\frac{\partial v_z}{\partial r} + \frac{v_\theta}{r}\frac{\partial v_z}{\partial \theta} + v_z\frac{\partial v_z}{\partial z}\right) = -\frac{\partial p}{\partial z} + \mu\left[\frac{1}{r}\frac{\partial}{\partial r}\left(r\frac{\partial v_z}{\partial r}\right) + \frac{1}{r^2}\frac{\partial^2 v_z}{\partial \theta^2} + \frac{\partial^2 v_z}{\partial z^2}\right] \qquad (3)$$

The physical boundary conditions used in plain microchannel for this investigation are given below:

$$v_z = 2 < v_{z=z_1} > \left[1 - \left(\frac{r}{r_0}\right)^2\right] \qquad z = z_1 \text{ (at the inlet of transition section)}$$
$$\text{and } p = p_{z_1}$$
$$v_r = 0, \ v_\theta = 0, \ v_z = 0 \qquad r = r_z \text{ (at the wall)}$$

On the basis of assumptions, boundary conditions, and other considerations, the axial and radial velocity profiles v_z, and v_r become

$$v_z = 2 < v_{z=z_1} > \left[\frac{r_0}{r_z}\right]^2 \left[1 - \frac{r^2}{r_z^2}\right] \qquad (4)$$

$$v_r = 2 < v_{(z=z_1)} > m\frac{r}{r_z}\left[\frac{r_0}{r_z}\right]^2 \left[1 - \frac{r^2}{r_z^2}\right] \qquad (5)$$

Comparing (4) and (5)

$$\frac{v_r}{v_z} = m\frac{r}{r_z} \qquad (6)$$

where $\frac{\partial r_z}{\partial z} = m = tan\emptyset$ is the slope of the converging and diverging wall.

The pressure drop in a converging–diverging section after simplification is as follows

$$\Delta p|_{ts} = \frac{16\mu v_{(z=z_1)}l}{r_0^2}\left[\frac{\varepsilon^2+\varepsilon+1}{3\varepsilon^2}+\frac{m^2(1+\varepsilon)}{2\varepsilon^5}\right] \qquad (7)$$

Further, the pressure drop in the plain microchannel is calculated using (8) after simplification is as follows:

$$\Delta p = \frac{16\mu v_{(z=0)}L}{r_0^2} \qquad (8)$$

The overall pressure drop is summation of pressure drop in plain microchannels part and transition sections. Finally, the pressure drop data obtained using above correlations will be compared with that from numerical simulation data.

III. NUMERICAL SIMULATIONS

A finite volume based CFD code FLUENT (ANSYS Academic Research CFD 15) that uses SIMPLE algorithm was used to solve the flow equations with associated boundary conditions in body fitted coordinate system. The physical realistic boundary conditions for this flow configuration in terms of 'CFD code terminology' are given below:

- The 'velocity inlet' boundary condition was imposed at the inlet boundary.
- The usual 'no slip conditions', i.e. $v_r = 0$, $v_\theta = 0$, $v_z = 0$ at the wall was imposed for liquid flow and first-order 'velocity slips conditions' at the wall for gas flow, expressed as.

$$r = r_0 \quad v_z|_{wall} = -\frac{2-\sigma_v}{\sigma_v}\lambda\frac{\partial v}{\partial r}|_{r=r_0}, \qquad v_r = 0$$

where σ_v is the tangential momentum accommodation coefficient, varying between 0 and 1 depending on the surface roughness, temperature and gas type. Here, $\sigma_v = 1$.

- The 'pressure outlet' boundary condition was applied at the exit boundary, and static gauge pressure was fixed to zero.

The entire microchannel length is taken as the computational domain to investigate the effect of transition section on the flow field. Because of converging-diverging shapes of the transition elements, tetrahedral meshes all over the computational domain are used as shown in Fig. 2. For each set of microchannel geometry, a fine mesh of 0.3 to 0.63 million cells with a minimum of 75 cells across the channel was built. Further, the grid refinement was applied near the solid-fluid interface to capture the boundary phenomena with greater resolution. The mesh independency test was performed to obtain refined grids. In grid independency test, it was found that a grid having 504500 elements is sufficient, and further refinement beyond this value does not influence velocity and pressure profiles at various cross-sections. The smallest control volumes were concentrated near the throat, where stresses and velocity gradients are expected to be higher. For stability of simulation results, second-order upwind discretization scheme was chosen, and convergence limit was set to 10^{-7} value of maximum residual tolerance.
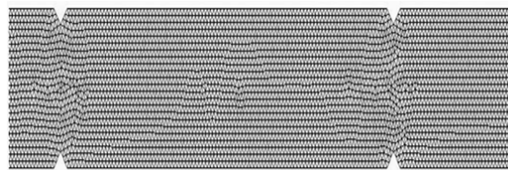

Fig. 2 Detail of the computational mesh used for simulation at *r-z* plane cross section

IV. RESULT AND DISCUSSION

Three dimensional numerical simulations were carried out on the microchannels presented in Table I using commercially available CFD code (FLUENT). The variations in local and total pressure, wall shear stress and forces acting in the microchannels were analyzed from the data obtained by both analytical and numerical techniques. The pressure drop was studied through simulation for water flow rate range of 0.5 to 20 m/s and for air flow rate range of 2 to 100 m/s. The effect of hydraulic diameter, type of transition section and fluid on pressure drop has also been studied.

A. Liquid Flow

The simulated and analytically obtained data for flow of incompressible fluid (water) in series of microchannel connected via transition section (MT-0, MT-1 and MT-2) have been presented and compared.

1. Variations of Pressure Drop in Microchannel

The pressure drop variation in a series of microchannel connected with transition section is shown in Figs. 3 (a)-(c). Each plot was for different size of microchannel specified therein. The pressure drop shows the linear variation with Reynolds number (*Re*) in microchannels along with plain microchannel. The microchannels connected via converging-diverging section with throat (MT-2) have higher pressure drop as compared to microchannels connected via converging-diverging section (MT-1). The pressure drops obtained in the microchannels are higher, approximately 5% for MT-1 and 10% for MT-2, than that of the plain microchannel (MT-0). These excessive pressure drops observed in the microchannels were due to imbalance between viscous and pressure forces in a transition section and thus responsible for acceleration and deceleration of the flow, which affect the overall pressure drop minutely in the microchannels connected via transition section. Figs. 3 (a)-(c) show that the pressure drops in the microchannels decrease with the increase in the channel diameter. The percentage difference in pressure drop observed between microchannels of diameter 100 and 184 μm was significantly high as compare to microchannels of diameter 184 and 249-μm channels, while the differences in diameter of the set of channels are approximately the same. This is because pressure drop is an inverse function of the second power of the hydraulic diameter for circular channel. In addition, the effect of type of transition section on pressure drop has also been numerically studied. It was observed that at low value of *Re*, pressure drop in converging-diverging section with and without throat were the same, but difference

604

in pressure drop increases with increase in *Re* and reaches towards the maximum, up to 50% for higher values of *Re*. This numerical observation is qualitatively in line with that

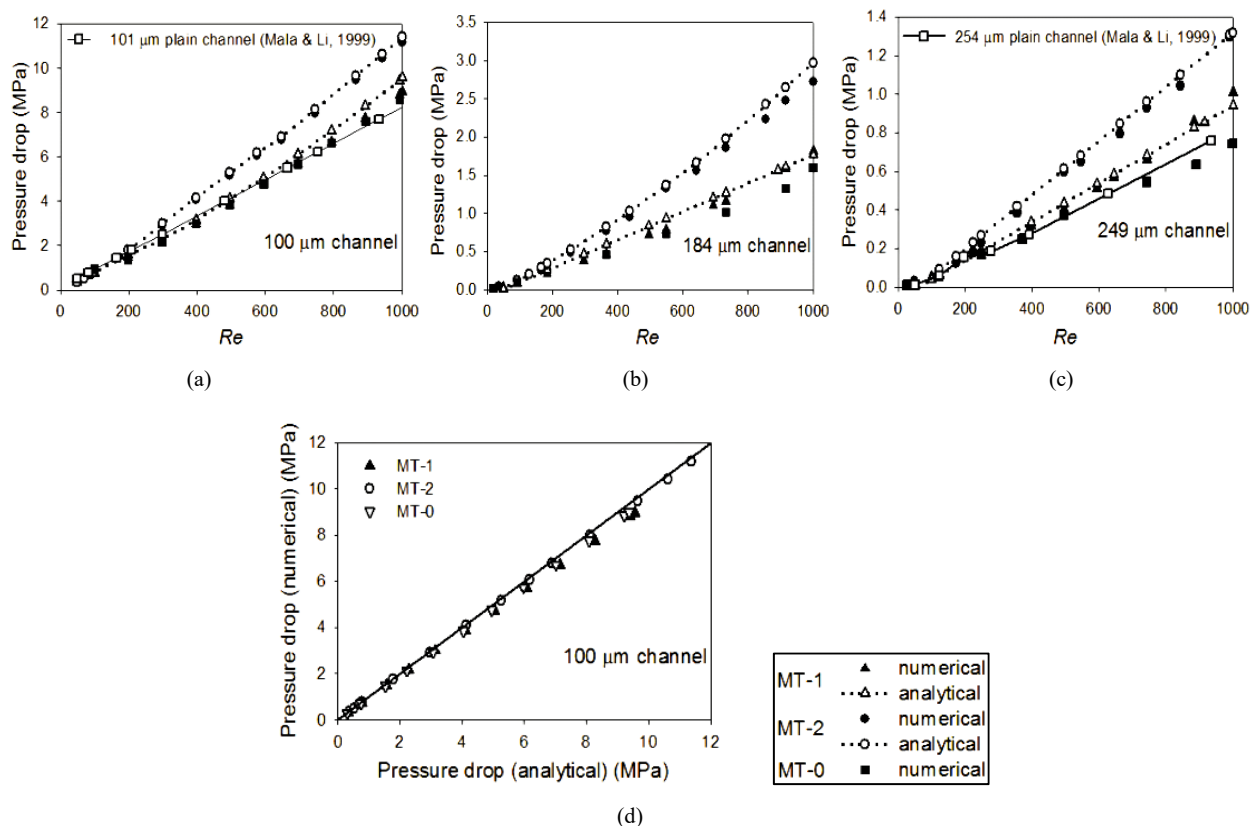obtained analytically along with experimental observations of [2] for plain microchannel.

Fig. 3 Pressure drop in the microchannels (MT-0, MT-1, and MT-2) (a) 100-μm channel (b) 184-μm channel (c) 249-μm channel (d) comparison between analytically and numerically obtained pressure drop

Fig. 3 (d) demonstrates the difference between the simulated and analytically predicted pressure drop in the microchannels connected via transition section as well as in the plain channel for *Re* range of 50-1000. The analytically calculated pressure drop was large compared to simulation results; this is because of variation in cross-sectional area which accommodated in pressure drop equation, and pressure gradient in the radial direction is neglected, whereas in simulation results, average hydraulic diameter was used to evaluate pressure difference.

The normalized pressure distribution along the centerline, (P/P_0) with the normalized length of transition section is shown in Fig. 4. It is clearly depicted from the figure that the variation of pressure along the centerline is nonlinear and shows a discontinuity in slope at the inlet and exit point of the transition section.

B. Gas Flow

Gas flow in microscale devices has some fundamental differences with respect to flow in the conventional macro-scale devices. This section deals with single phase gas flow in microchannels (MT-0, MT-1 and MT-2).

1. Variations of Pressure Drop in Microchannel

Similar observations were observed for gas flow in the microchannel as shown in Fig. 5. The large pressure drops in the microchannels MT-1 and MT-2 are due to acceleration and deceleration of flow in the transition section along with frictional losses. Under fully developed condition, pressure force was exactly balanced by the viscous force in the plain microchannel, whereas in a transition section viscous force shows dominance at low value of Reynolds number due to rarefaction effect. However, pressure force was dominant at higher value of Reynolds number due to compressibility effect along with acceleration and deceleration of the flow.

It is seen from Fig. 6 that the pressure distribution exhibits a nonlinear behavior due to the compressibility effect and shows a discontinuity in slope at the inlet and exit point of the transition section. The nonlinear pressure distribution in straight channel is due to the effects of the compressibility and rarefaction [15], whereas the large pressure difference in the transition section results is due to contraction and expansion of the fluid leading to acceleration and deceleration of the flow. These two opposing effects result in a nonlinear pressure distribution. The deviations of the pressure distribution from

the linear distribution decrease with an increase in Knudsen number.
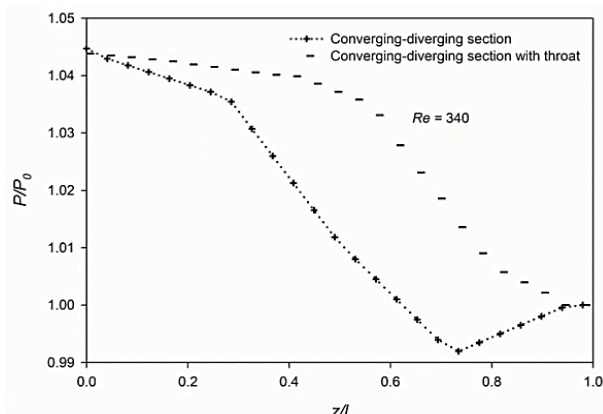

Fig. 4 Pressure distributions along the centerline in both type of different transition sections for water flow in 100-μm microchannels

2. Knudsen and Mach Number Distribution

Microscale gas flow-separation in the transition sections was investigated for two Reynolds numbers 342 and 547. Fig. 7 shows the variation of Knudsen number at centerline for both the cases. It can be seen from the figure that the distribution of Knudsen number in the converging-diverging section with and without throat follows the variation similar to velocity distribution in the transition section. The Knudsen number varies along the length of transition section. The computed Knudsen numbers for Reynolds number 547 is lower than that for 342 which indicates that the compressibility is a dominating factor. Further, relatively high Mach numbers in the range of 0.1 to 1.2 were achieved in the transition section for lower value of Reynolds numbers.

The Mach number contour (Reynolds number = 547) for transition sections and plain channel case is illustrated in Figs. 8 (a)-(c). It can be seen from the figures that Mach number varies nonlinearly in the transition sections and in the plain channel. This nonlinear variation is in accordance with the nonlinear pressure distribution, which also indicates that the compressibility is a dominating factor in the transition section as well as in the plain microchannel. In the transition section, a higher value of Mach number was observed near the junction or throat of converging-diverging section, this clearly shows that the flow separation occurs in the transition section.
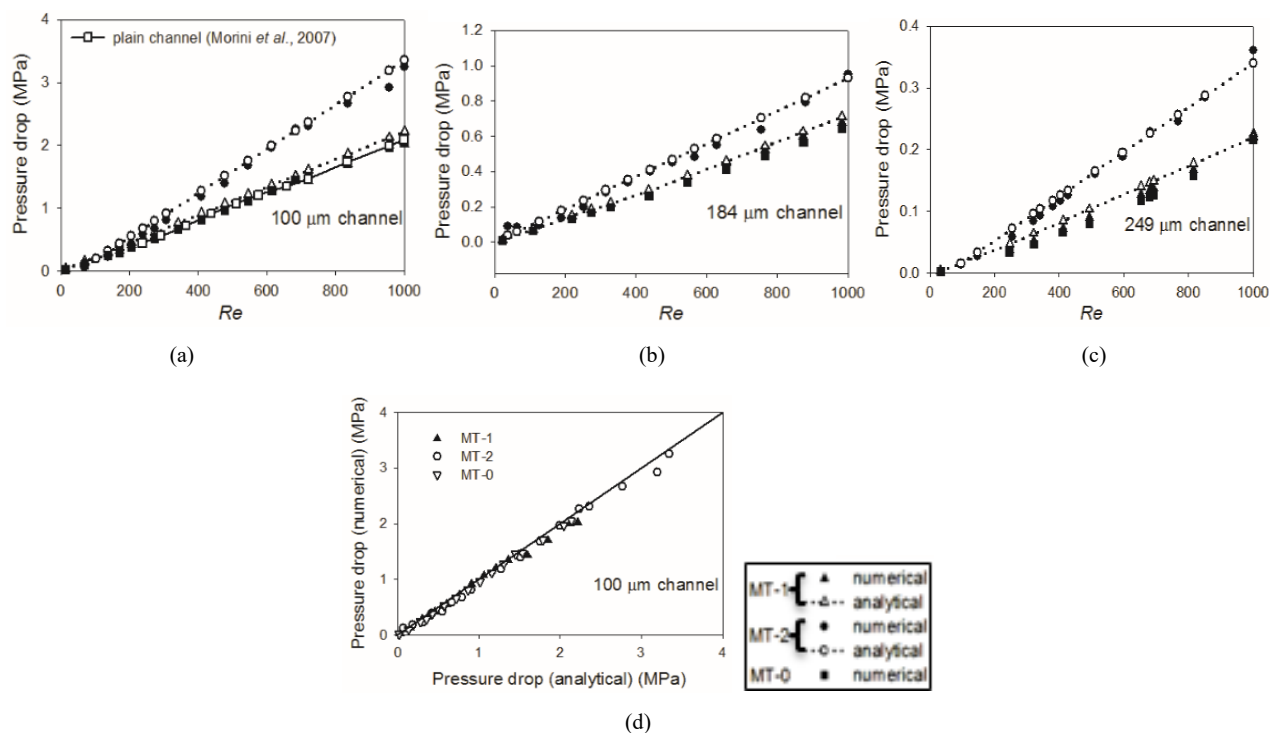

(a)

(b)

(c)

(d)

Fig. 5 Pressure drop in the microchannel (MT-0, MT-1, and MT-2) (a) 100-μm channel (b) 184-μm channel (c) 249-μm channel (d) comparison between analytically and numerically obtained pressure drop
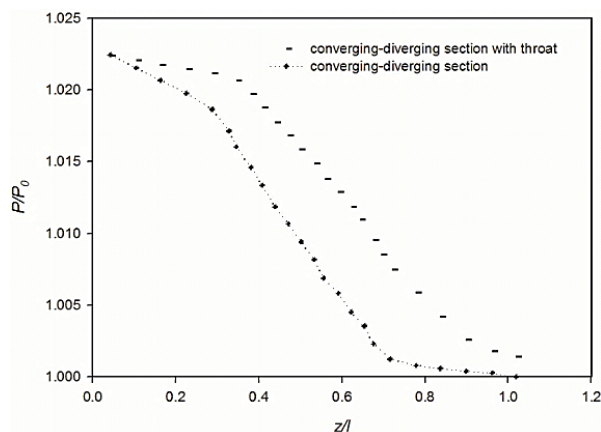
Fig. 6 Pressure distributions along the centerline in both type of different transition sections for air flow in 100-μm microchannels
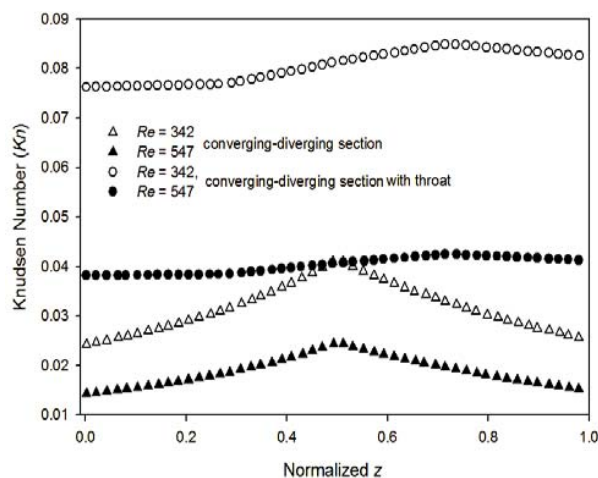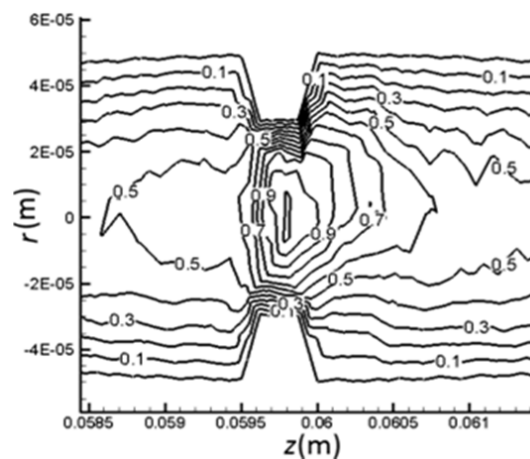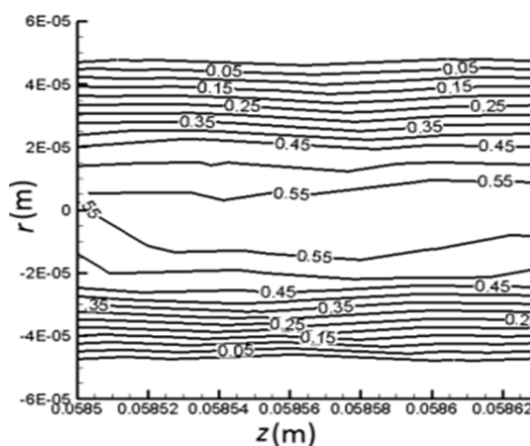

Fig. 7 Variation in Knudsen number along the centerline ($r = 0$, $\theta = 0$) for 100 μm channel
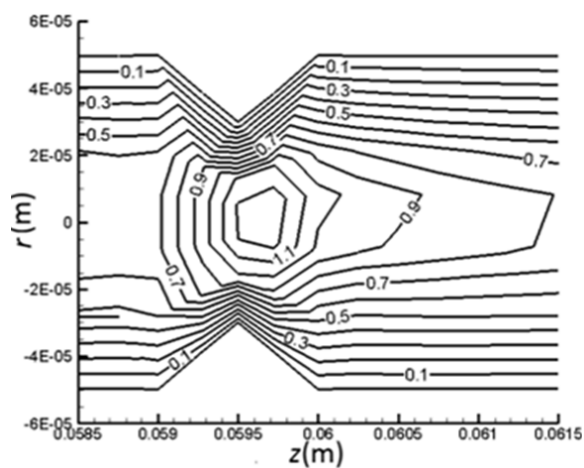

(b)

(c)

Fig. 8 Mach number distribution for $Re = 547$ (a) converging-diverging section (b) converging-diverging section with throat (c) uniform cross-section

(a)

V. CONCLUDING REMARKS

In this investigation, the analytical and numerical studies were carried out on series of microchannels connected through transition sections viz. MT-1 and MT-2. The obtained results show good agreement with the analytical results along with the experimental data due to other investigators. The pressure drops in the series of microchannels, i.e. MT-1 and MT-2, are higher than that of the plain microchannel (MT-0) for both air flow and water flow for the Reynolds number range 50-1000. The non-linear pressure distribution along the centerline, (P/P_0) was observed in both type of transition section. For water flow, this was due to acceleration and deceleration, whereas for gas flow this behavior was due to effects of the compressibility and rarefaction.

The present work shows that the converging-diverging transition section is far superior to the converging–diverging section with throat, and this configuration can be used in enhancement of transport processes.

607

REFERENCES

[1] M. Gad-el-Hak, "The fluid mechanics of microdevices—the Freeman Scholar lecture". *ASME J. Fluids Eng.*, vol. 21, pp 5–33, 1999.

[2] G. M. Mala, D. Li, "Flow characteristics of water in microtubes" *Int. J. Heat Fluid Flow* vol. 20, pp 142–148 1999.

[3] R. W. Barber, D. R. Emerson, "Challenges in modeling gas-phase flow in microchannels: form slip to transition" *Heat Transfer Eng.* vol. 27, pp 3–12, 2006.

[4] B. Verma, A. Demsis, A. Agrawal, S. V. Prabhu, "Semi-empirical correlation for the friction factor of gas flowing through smooth microtubes" *J. Vac. Sci. Technol. A* vol. 27, pp 284–290, 2009a.

[5] A. Agrawal, "A comprehensive review on gas flow in microchannel" *Int. J. Micro Nano Scale Transp.* vol. 2, pp 1–40, 2011.

[6] S. Y. K. Lee, M. Wong, Y. Zohar, "Pressure losses in microchannels with bends" *Proc. 14th Intl. Micro Electro Mech. Systems Conf. MEMS'01*, pp 491- 494, 2001a.

[7] W. Y. Lee, S. Y. K. Lee, M. Wong, Y. Zohar, "Microchannels in series with gradual contraction/expansion" *Proc. Intl. Mech. Eng. Congr. & Exposition, MEMS 2*, pp 467-472, 2000.

[8] X. Li, W. Y. Lee, M. Wong, Y. Zohar, "Gas flow in constriction microdevices" *Sensors Actuat.* vol. A83, pp 277-283, 2000.

[9] W. Y. Lee, M. Wong, Y. Zohar, "Flow separation in constriction microchannels" *Proc. 14th Intl. Micro Electro Mech. Systems Conf. MEMS'01*, pp 495-498, 2001b.

[10] S. Y. K. Lee, M. Wong, Y. Zohar, "Characterization of a mixing layer microdevice" *Proc. 11th Intl. Conf. Solid-State Sensors and Actuators, Transducers'01*, pp 1206-1209, 2001c.

[11] W. Ehrfeld, K. Golbig, V. Hessel, H. Lowe, T. Richter, "Characterization of mixing in micromixer by a test reaction: Single mixing units and mixer arrays" *Ind. Eng. Chem. Res.* vol. 38, pp 1075-1082, 1999.

[12] D. V. Boger, "Viscoelastic Flows through Contractions" *Ann. Rev. of Fluid Mech.* vol. 19, pp 157-182, 1987

[13] S. A. White, A. D. Gotsis, D. G. Baird, "Review of the Entry Flow Problem – Experimental and Numerical" *J. of Non-Newtonian Fluid Mech.* vol. 24, 121-160, 1987.

[14] W. Y. Lee, S. Y. K. Lee, M. Wong, Y. Zohar, "Microchannels in series connected via a contraction/expansion section" *J. Fluid Mech.* vol. 459, pp 187-206, 2002.

[15] A. Besbob, "validation of a new velocity slip model for separated gas microflows" *Heat Transfer, Part B: Fundamentals: An International Journal of Computation and Methodology*, vol. 40, no.6, pp. 451-471, 2000.